

Fibrillar fibronectin plays a key role as nucleator of collagen I polymerization during macromolecular crowding-enhanced matrix assembly

Jenna Graham¹, Michael Raghunath², Viola Vogel^{1*}

Author affiliations:

- 1- Department of Health Sciences and Technology, ETH Zürich, CH-8093 Zürich, Switzerland
- 2- ZHAW School of Life Sciences and Facility Management, Institute for Chemistry and Biotechnology, Center for Cell Biology and Tissue Engineering, CH-8820 Wädenswil, Switzerland

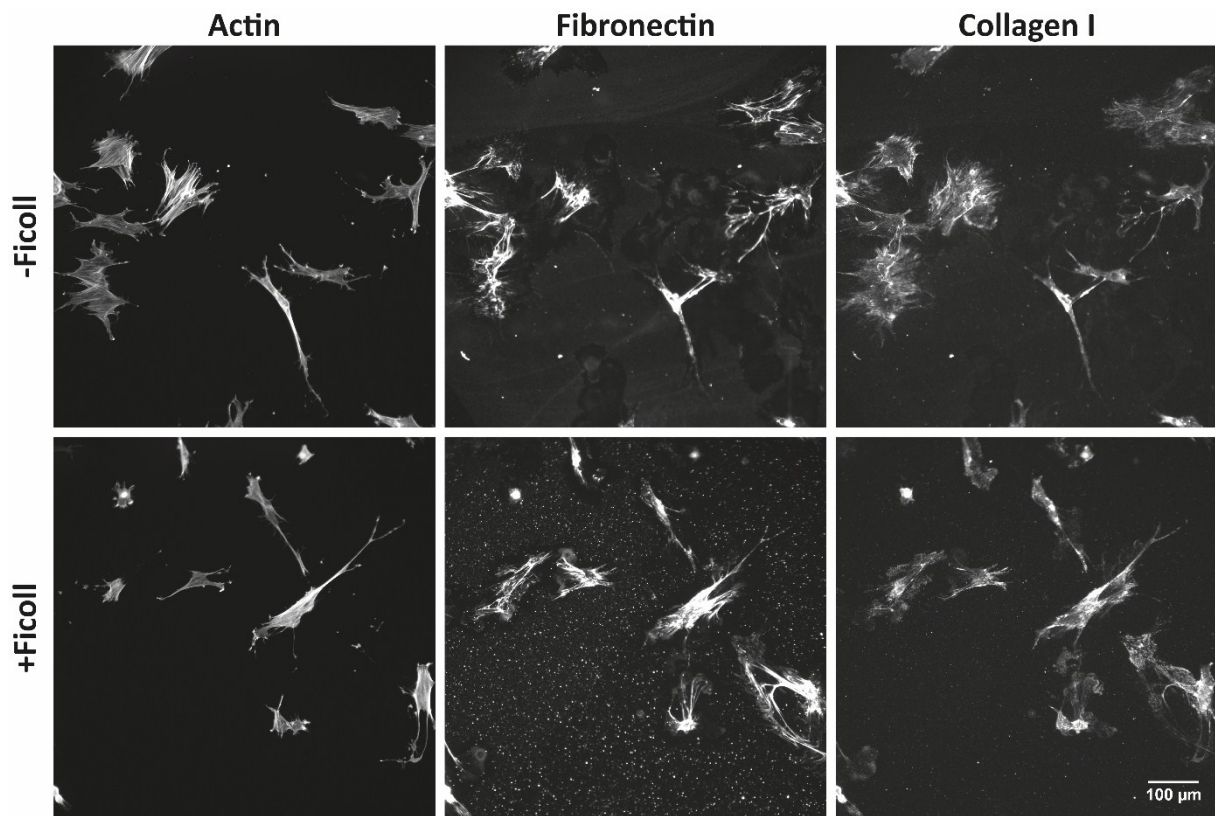
* corresponding author (viola.vogel@hest.ethz.ch)

Supplemental movie 1: Time-lapse widefield microscopy movie showing how fibroblasts harvest fibronectin adsorbed to the glass substrate. The left panel shows fibroblasts in phase contrast and the right panel shows the Alexa-546 labeled fibronectin coating. The glass was coated with 100µg/mL Alexa-546 labeled fibronectin for one hour before cell seeding. Human skin fibroblasts were seeded at 4,000 cells/cm² and allowed to adhere 24 hours before media was changed to containing Ficoll (37.5mg/mL 70kDa + 25mg/mL 400kDa). Movie acquisition started approximately one hour after media change. Since the movie starts approximately 24 hours after cell seeding, some of the coating has already been scraped off at the start of acquisition. The movie captures 10 hours of cell culture. Cells can be seen migrating, scraping off the coating, and dividing. Note that two cell rounding and division events were captured here, during which the cells did not scrape off fibronectin.

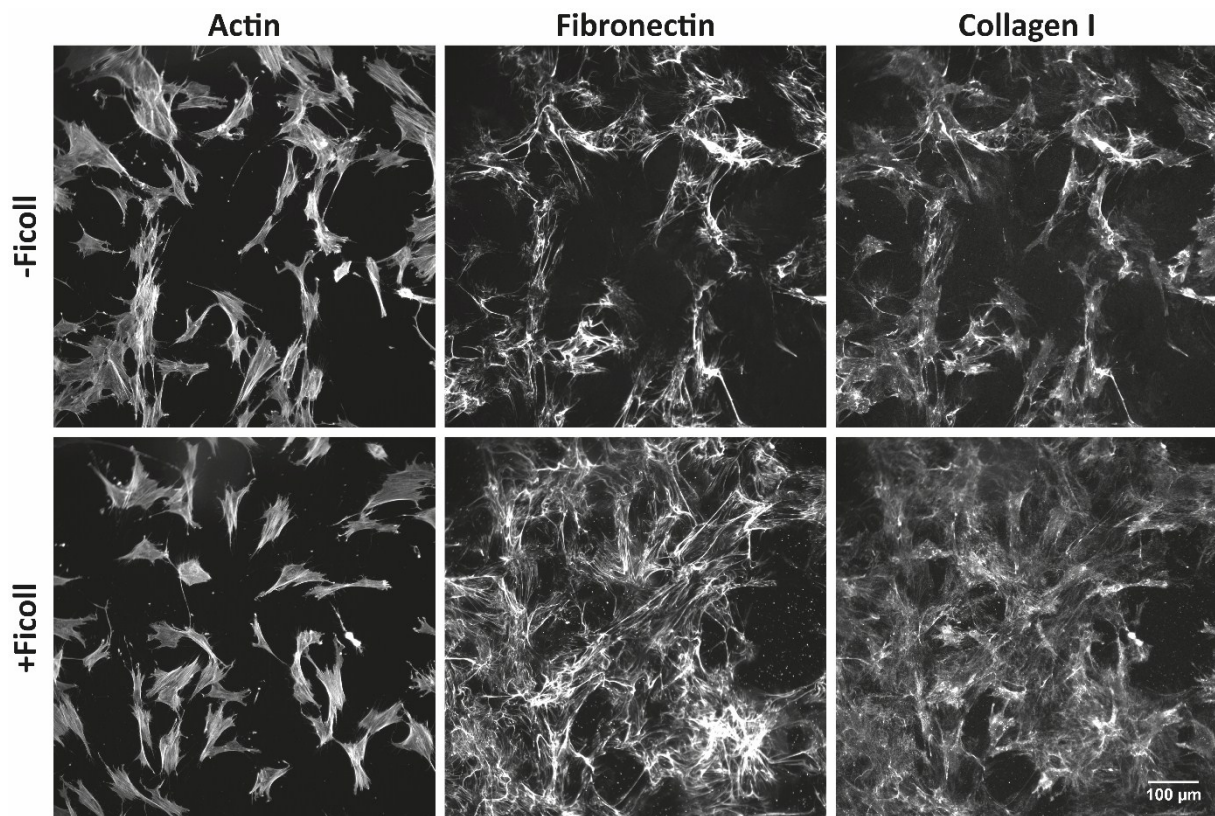
Supplemental movie 2: Single widefield fluorescence image of matrix assembled in 16 hours in the presence of Ficoll. Different channels are turned on and off to show proximity of fibronectin (red) and collagen I (green). Images are from the same data set used for main text Figure 1.

Supplemental movie 3: Single widefield fluorescence image of matrix assembled in 2 days in the presence of Ficoll. Different channels are turned on and off to show proximity of fibronectin (red) and collagen I (green). Images are from the same data set used for main text Figure 2.

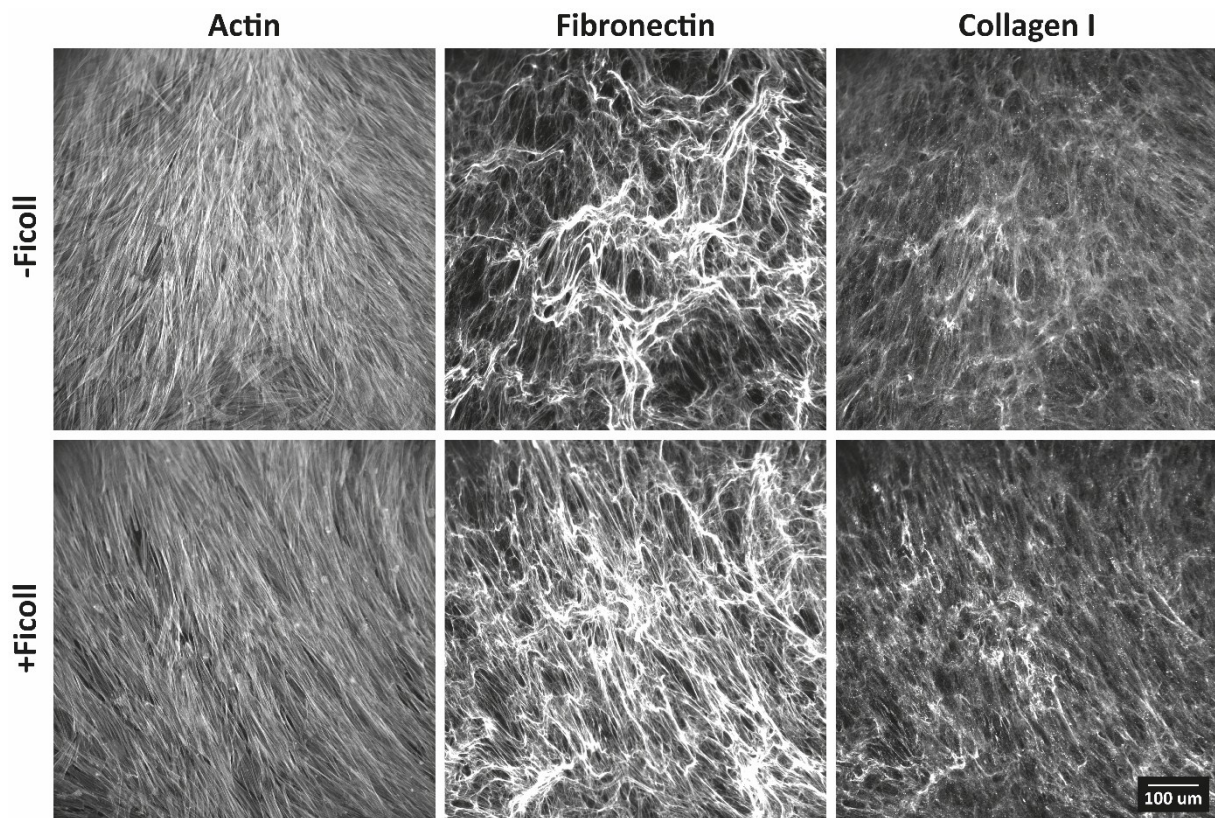
Supplemental movie 4: Confocal z-stack of matrix produced in 6 days without and with Ficoll. The top row shows -Ficoll and the bottom row shows +Ficoll. Fibronectin and collagen I are shown side-by-side for each condition. The z-stack repeats 4 times. Z-step = 1µm. The images are from a different experiment, but with the same conditions as the data set used for main text Figure 3.



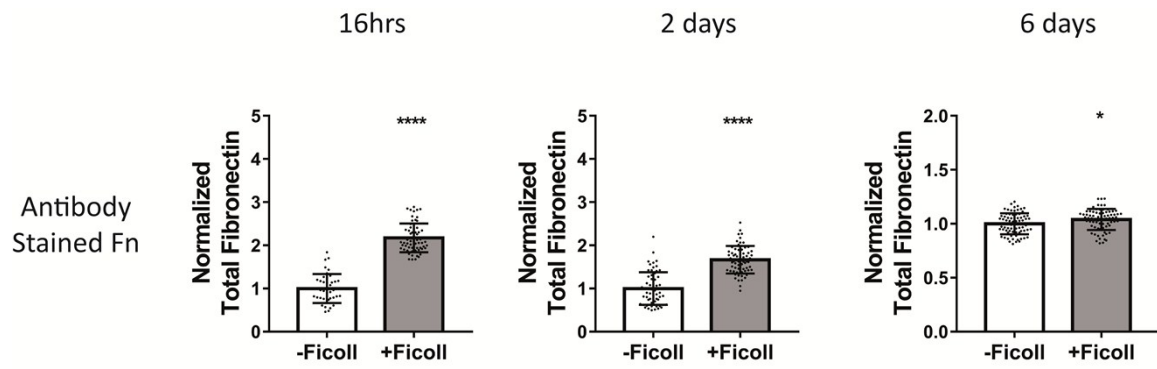
Supplemental figure 1: Widefield greyscale images captured with a 20x objective of cells and matrix assembled in 16 hours +/-Ficoll (37.5mg/mL 70kDa + 25mg/mL 400kDa). Images are from the same data set used for main text Figure 1. Glass substrates preadsorbed with 50µg/mL plasma fibronectin (10% Alexa-647-labeled). Cells cultured in MEM Alpha supplemented with 10% fetal bovine serum, 1% penicillin-streptomycin, 100µM L-ascorbic acid 2-phosphate, and 50µg/mL plasma fibronectin (10% Alexa-647-labeled).



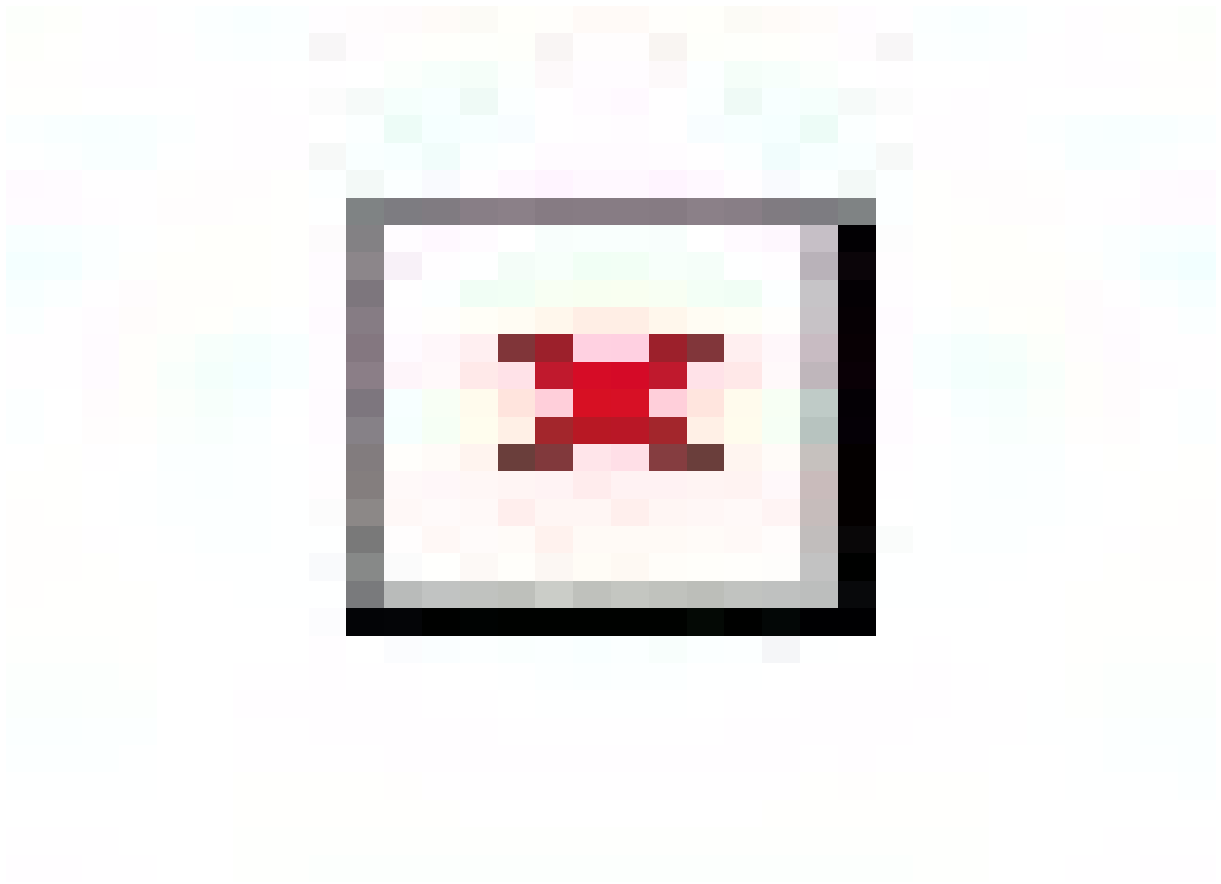
Supplemental figure 2: Widefield greyscale images captured with a 20x objective of cells and matrix assembled in 2 days +/-Ficoll (37.5mg/mL 70kDa + 25mg/mL 400kDa). Images are from the same data set used for main text Figure 2. Glass substrates preadsorbed with 50μg/mL plasma fibronectin (10% Alexa-647-labeled). Cells cultured in MEM Alpha supplemented with 10% fetal bovine serum, 1% penicillin-streptomycin, 100μM L-ascorbic acid 2-phosphate, and 50μg/mL plasma fibronectin (10% Alexa-647-labeled).



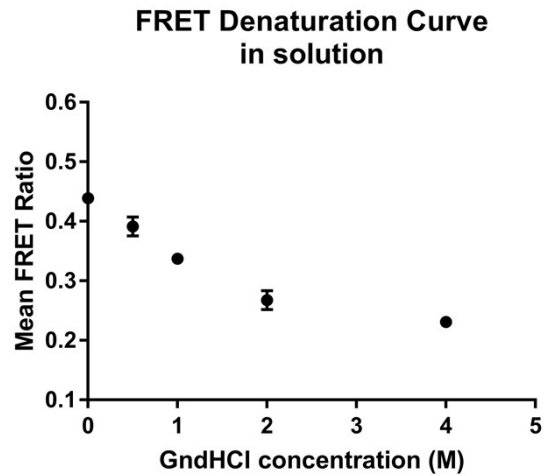
Supplemental figure 3: Widefield greyscale images captured with a 20x objective of cells and matrix assembled in 6 days +/-Ficoll (37.5mg/mL 70kDa + 25mg/mL 400kDa). Images are from the same data set used for main text Figure 3. Glass substrates preadsorbed with 50 μ g/mL plasma fibronectin (10% Alexa-647-labeled). Cells cultured in MEM Alpha supplemented with 10% fetal bovine serum, 1% penicillin-streptomycin, 100 μ M L-ascorbic acid 2-phosphate, and 50 μ g/mL plasma fibronectin (10% Alexa-647-labeled).



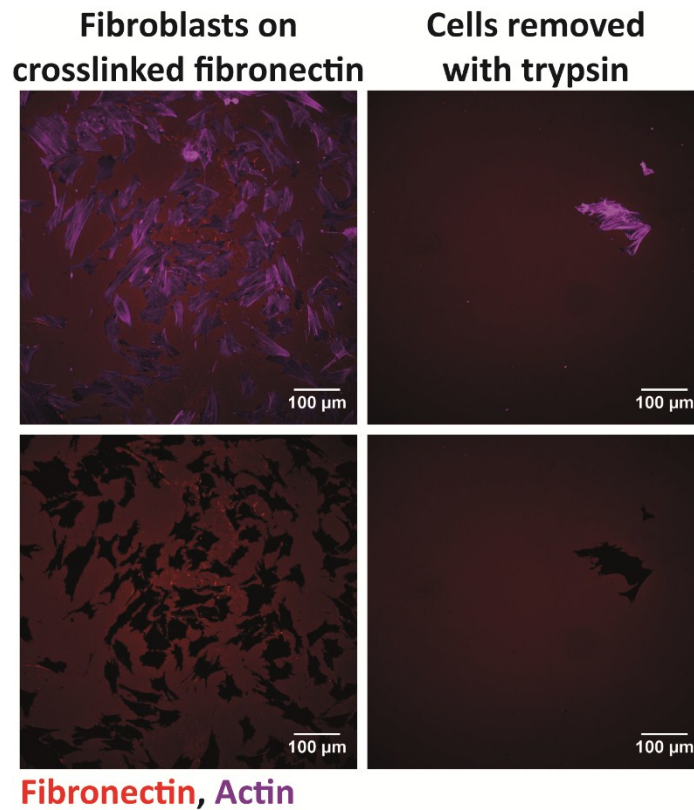
Supplemental figure 4: Fibronectin matrix assembly quantified by antibody staining. Reported values are the summed intensity of fibronectin fluorescence signal, normalized to the average in -Ficoll control. See main text Figures 1-3 for comparable quantification with Alexa 647-fibronectin. * indicates $p < 0.05$, **** indicates $p < 0.0001$



Supplemental figure 5: Fibronectin on the glass surface after 2 days culture +/-Ficoll, both with and without 50 μ g/mL human plasma fibronectin supplemented to the medium. Reported values are the summed intensity of fibronectin antibody-stain divided by the area. *** indicates $p < 0.001$, **** indicates $p < 0.0001$. Same data set as shown in main text Figure 5.



Supplemental figure 6: Fibronectin-FRET denaturation curve. The Fn-FRET probe was gradually denatured in increasing concentrations of the chemical denaturant guanidine hydrochloride and the FRET ratio was measured in solution. Reported values are the average FRET ratio for 5 individual measurements at each concentration of GdnHCl. See main text Figure 6.



Supplemental figure 7: In order to confirm that the dark areas in the fibronectin channel on cross-linked fibronectin coating are shadows from the cells rather than digested or harvested coating (see main text Figure 7), one sample was treated with trypsin before fixing and staining. The sample was otherwise treated the same as all others. On the left is a standard sample with cells, and on the right is a sample where cells have been removed by trypsin (except for one that remained adherent). The top images show both cells and fibronectin, whereas the bottom images show only the fibronectin channel. The fact that all dark areas in the fibronectin channel disappeared with trypsin treatment (except the one where a cell remained) confirms that the cross-linked coating is still intact and the dark areas are places where the fibronectin antibody could not access the coating.

Supplemental table 1: Summary of literature related to the use of crowding to enhance matrix assembly.

Cell/Tissue Type	Crowder	Key Findings	Reference
Human fibroblasts	500kDa Dextran Sulfate (DxS) 100 µg/mL	<ul style="list-style-type: none"> – Conversion of unprocessed procollagen in media to collagen in matrix – No impact of neutral Dextran at 100µg/mL 	Lareu et al., Tissue Eng. (2007)(1)
Human lung fibroblasts	500kDa DxS 100µg/mL 200kDa polysodium-4-styrene sulfonate (PSS) 100µg/mL	<ul style="list-style-type: none"> – Accelerated activity of procollagen C-proteinase – Effective in 2D and 3D (2D>>3D) – No impact of 70kDa Ficoll, 400kDa Ficoll at 50mg/mL, or 10kDa DxS at 100ug/mL – Hydrodynamic radius and charge of crowder affect result 	Lareu et al., FEBS Letters (2007)(2)
Human lung fibroblasts	500kDa DxS 100µg/mL Ficoll mixture (37.5mg/mL 70kDa + 25mg/ml 400kDa)	<ul style="list-style-type: none"> – Used crowding to create an <i>in vitro</i> fibrosis model to screen antifibrotic compounds – Faster, more granular matrix assembly with DxS than Ficoll 	Chen et al., Br. J. Pharmacol. (2009)(3)
Several cell types	500kDa DxS 100µg/mL Ficoll mixture	<ul style="list-style-type: none"> – Assembly of many ECM components increased by DxS 	Chen et al., Adv. Drug Deliv. Rev. (2011)(4)
Human lung fibroblasts	500kDa DxS 100µg/mL	<ul style="list-style-type: none"> – Matrix assembled by fibroblasts with crowding supported stable propagation of human embryonic stem cells better than Matrigel 	Peng et al., J. Tissue Eng. Regen. M. (2012)(5)
Human mesenchymal stem cells	Ficoll mixture	<ul style="list-style-type: none"> – Increased matrix assembly, alignment – Feedback to cells: cytoskeletal alignment, increased adhesion, proliferation 	Zeiger et al., PLoS One (2012)(6)
Porcine chondrocytes	Ficoll mixture	<ul style="list-style-type: none"> – Increased collagen and glycosaminoglycan production in 2D but not in 3D model (PGA unweaved fibers) 	Chen et al., Tissue Eng. Part C (2013)(7)
Human corneal, lung, and dermal fibroblasts	Caregeenan type 1 (CR) 75µg/mL	<ul style="list-style-type: none"> – Increased collagen I and fibronectin deposition by all cell types. Degree of effect was cell type dependent. 	Kumar et al., Adv. Sci. Tech. (2014)(8)
MSCs			

Human MSCs	Ficoll mixture	<ul style="list-style-type: none"> – Enhanced adipogenic differentiation (chemically induced): more lipid production, more ECM – Adipo-ECM generated under crowding also promoted enhanced differentiation 	Ang et al., Tissue Eng. Part A (2014)(9)
Human fibroblasts MSCs	Polyvinyl pyrrolidone (PVP)	<ul style="list-style-type: none"> – PVP has a similar ECM enhancing effect as Ficoll but can achieve higher FVO without increased viscosity. 	Rashid et al., Tissue Eng. Part C (2014)(10)
Human lung fibroblasts, tenocytes, osteoblasts	500kDa DxS 100µg/mL CR 75µg/mL	<ul style="list-style-type: none"> – Low serum (0.5%) resulted in higher collagen I production with crowding – Generated cell-sheet that could be released from pNIPAAm substrate – Many matrix components enhanced by CR 	Satyam et al., Adv. Mater. (2014)(11)
Cell-free collagen gel formation	400kDa Ficoll 0-25mg/mL	<ul style="list-style-type: none"> – Rate of collagen nucleation and fiber growth can be tuned by crowding level resulting in altered fiber diameter and organization 	Dewavrin et al., Acta. Biomater. (2014)(12)
Bovine vascular endothelial cells	Ficoll mixture	<ul style="list-style-type: none"> – Greater amount of collagen IV produced, more aligned 	Liu et al., Meter. Res. Soc. Symp. Proc. (2014)(13)
Rat vocal fold fibroblasts	Ficoll mixture	<ul style="list-style-type: none"> – Increased collagen I assembly with crowding and TGFβ-1, toward the goal of <i>in vitro</i> fibrosis drug screening 	Graupp et al., Laryngoscope (2014)(14)
Human corneal fibroblasts	Ficoll mixture	<ul style="list-style-type: none"> – Production of a cell-sheet that could be released from temperature responsive polymer in 6 days – No change in ECM gene expression or αSMA expression – Effective in medium containing both bovine and human serum 	Kumar et al., Sci. Rep. (2015)(15)
Cell-free collagen gel formation	40kDa and 360kDa PVP 70kDa and 200kDa Dextran 70kDa and 400kDa Ficoll	<ul style="list-style-type: none"> – Mixtures of different size crowders have a synergistic effect that results in higher volume exclusion than the simple sum of hydrodynamic radii 	Dewavrin et al., J. Phys. Chem. B (2015)(16)
Human corneal fibroblasts	500kDa DxS 100µg/mL CR 75ug/mL	<ul style="list-style-type: none"> – Similar matrix enhancing effect of DxS and CR – DxS caused some changes in gene expression toward myofibroblast, whereas CR didn't 	Kumar et al., Tissue Eng. Part C (2015)(17)

Human MSCs	Ficoll mixture + 10kDa DxS 100µg/mL	<ul style="list-style-type: none"> – Produced ECM that retained glycosaminoglycans and growth factors and supported hematopoietic stem and progenitor cell expansion 	Prewitz et al., Biomaterials (2015)(18)
Organotypic skin culture (human keratinocytes and fibroblasts)	Ficoll mixture	<ul style="list-style-type: none"> – Improved organotypic coculture with crowding, improved ECM assembly and promoted formation of a collagen VII-rich dermal-epidermal junction 	Benny et al., Tissue Eng. Part A (2015)(19)
Human bone-marrow MSCs (bmMSCs)	Ficoll mixture	<ul style="list-style-type: none"> – Enhanced brown-adipocyte differentiation as well as “browning” of bmMSC-derived white adipocytes, attributed to MMC induced 3D ECM that encapsulated cells 	Lee et al., Sci. Rep. (2016)(20)
Human dermal fibroblasts	CR 75µg/mL	<ul style="list-style-type: none"> – Optimized oxygen tension and serum concentration in culture with CR: 2% oxygen tension and 0.5% serum lead to the most matrix with CR 	Satyam et al., Acta. Biomater. (2016)(21)
Human bmMSCs	CR 75µg/mL	<ul style="list-style-type: none"> – CR enhanced matrix assembly at both 2% and 20% oxygen tension – Matrix gene expression, surface markers, and transcription factors not affected – Differentiation potential was sensitive to oxygen tension and crowding 	Cigognini et al., Sci. Rep. (2016)(22)
Human corneal fibroblasts	CR 75µg/mL	<ul style="list-style-type: none"> – Optimized oxygen tension and serum concentration in culture with CR: 2% oxygen tension and 0.5% serum lead to the most matrix with CR 	Kumar et al., J. Tissue Eng. Regen. M. (2017)(23)
Adipose stem cells	Ficoll mixture	<ul style="list-style-type: none"> – Osteogenesis and adipogenesis enhanced by MMC, chondrogenesis inhibited in medium with human or bovine serum – MMC was not beneficial in xeno-free/serum-free medium 	Patrikoski et al., Stem Cells Int. (2017)(24)
Reconstituted porcine kidney matrix	400kDa Ficoll	<ul style="list-style-type: none"> – Crowding level modulated the fibrillation kinetics and matrix architecture, as well as distribution of ECM components 	Magno et al., Acta Biomater. (2017)(25)
Drop-on-demand bioprinting	PVP	<ul style="list-style-type: none"> – Controlled the architecture of bioprinted collagen hydrogel with PVP, could vary architecture within gel 	Ng et al., Biomater. Sci. (2018)(26)
Human chondrocytes	CR 100µg/mL	<ul style="list-style-type: none"> – Some benefit of MMC in chondrocyte culture, but not as much as other cell types 	Graceffa et al., J. Tissue Eng. Regen. M. (2019)(27)

Human dermal fibroblasts	CR Ficoll DxS	– Tested several different cocktails of crowders with different components and molecular weight, found polydispersity and negative charge to be important factors driving matrix assembly	Gaspar et al., Acta Biomater. (2019)(28)
--------------------------	---------------------	---	--

Supplemental table 2: Summary of findings regarding the effect of Ficoll on the amount of collagen I matrix at late timepoints. Only studies with standard Ficoll mixture (37.5mg/mL 70kDa + 25mg/mL 400kDa) as the crowder and supplemental ascorbic acid in culture media were included. Entries without references specified are from the same study as the row above.

Protein	Cell type	Crowder	Time point	Fold change in collagen	Method	Reference
Collagen I	Dermal fibroblasts	Ficoll	7 days	No change	SDS-PAGE of pepsin digested cell layers	Gaspar et al., Acta Biomater. (2019)(28)
			14 days	1.3x		
Collagen I	Dermal fibroblasts	Ficoll	6 days	Increased (fold-change not clear)	Immunofluorescence, thresholded area of matrix normalized to cell count	Rashid et al. Tissue Eng. Part C (2014)(10)
	Mesenchymal stem cells		>5x			
Total collagen	Mesenchymal stem cells	Ficoll + dextran sulfate	10 days	0.5x	Sircol assay of pepsin digested decellularized ECM layers	Prewitz et al., Biomaterials (2015)(18)
Collagen I	Mesenchymal stem cells	Ficoll	7 days	No change	SDS-PAGE of pepsin digested cell layers	Cigognini et al., Sci. Rep. (2016)(22)
			14 days	No change		
Collagen I	Corneal fibroblasts	Ficoll	6 days	>3x	SDS-PAGE of pepsin digested media and cell layers	Kumar et al. Sci. Rep. (2015)(15)

References

1. Lareu RR, Arsianti I, Subramhanya HK, Yanxian P, Raghunath M. In vitro enhancement of collagen matrix formation and crosslinking for applications in tissue engineering: a preliminary study. *Tissue Eng.* 2007;13(2):385–91.
2. Lareu RR, Subramhanya KH, Peng Y, Benny P, Chen C, Wang Z, et al. Collagen matrix deposition is dramatically enhanced in vitro when crowded with charged macromolecules: The biological relevance of the excluded volume effect. *FEBS Lett.* 2007 Jun 12;581(14):2709–14.
3. Chen CZ, Peng YX, Wang ZB, Fish P V, Kaar JL, Koepsel RR, et al. The Scar-in-a-Jar: studying potential antifibrotic compounds from the epigenetic to extracellular level in a single well. *BrJPharmacol.* 2009;158(5):1196–209.
4. Chen C, Loe F, Blocki A, Peng Y, Raghunath M. Applying macromolecular crowding to enhance extracellular matrix deposition and its remodeling in vitro for tissue engineering and cell-based therapies. *Adv Drug Deliv Rev.* 2011 Apr 30;63(4–5):277–90.
5. Peng Y, Bocker MT, Holm J, Toh WS, Hughes CS, Kidwai F, et al. Human fibroblast matrices bio-assembled under macromolecular crowding support stable propagation of human embryonic stem cells. *J Tissue Eng Regen Med.* 2012 Nov;6(10):e74-86.
6. Zeiger AS, Loe FC, Li R, Raghunath M, Van Vliet KJ. Macromolecular crowding directs extracellular matrix organization and mesenchymal stem cell behavior. *PLoS One.* 2012 Jan 23;7(5):e37904.
7. Chen B, Wang B, Zhang WJ, Zhou G, Cao Y, Liu W. Macromolecular crowding effect on cartilaginous matrix production: a comparison of two-dimensional and three-dimensional models. *Tissue Eng Part C Methods.* 2013 Aug 20;19(8):586–95.
8. Kumar P, Satyam A, Gaspar D, Cigognini D, Sanz-Nogués C, O'Brien T, et al. Macromolecular Crowding: The Next Frontier in Tissue Engineering. *Adv Sci Technol.* 2014 Oct 31;96:1–8.
9. Ang XM, Lee MHC, Blocki A, Chen C, Ong LLS, Asada HH, et al. Macromolecular crowding amplifies adipogenesis of human bone marrow-derived mesenchymal stem cells by enhancing the pro-adipogenic microenvironment. *Tissue Eng Part A.* 2014 Mar 28;20(5–6):966–81.
10. Rashid R, Lim NSJ, Chee SML, Png SN, Wohland T, Raghunath M. Novel Use for Polyvinylpyrrolidone as a Macromolecular Crowder for Enhanced Extracellular Matrix Deposition and Cell Proliferation. *Tissue Eng Part C Methods.* 2014 Dec 2;20(12):994–1002.
11. Satyam A, Kumar P, Fan X, Gorelov A, Rochev Y, Joshi L, et al. Macromolecular crowding meets tissue engineering by self-assembly: a paradigm shift in regenerative medicine. *Adv Mater.* 2014 May 21;26(19):3024–34.
12. Dewavrin J-Y, Hamzavi N, Shim VPW, Raghunath M. Tuning the architecture of three-dimensional collagen hydrogels by physiological macromolecular crowding. *Acta Biomater.* 2014 Oct;10(10):4351–9.
13. Liu FD, Zeiger AS, Van Vliet KJ. Time-Dependent Extracellular Matrix Organization and Secretion from Vascular Endothelial Cells due to Macromolecular Crowding. *MRS Proc.* 2014 Jan 1;1623:mrsf13-1623-f02-10.

14. Graupp M, Gruber H-J, Weiss G, Kiesler K, Bachna-Rotter S, Friedrich G, et al. Establishing principles of macromolecular crowding for in vitro fibrosis research of the vocal fold lamina propria. *Laryngoscope*. 2015 Jun;125(6):E203–9.
15. Kumar P, Satyam A, Fan X, Collin E, Rochev Y, Rodriguez BJ, et al. Macromolecularly crowded in vitro microenvironments accelerate the production of extracellular matrix-rich supramolecular assemblies. *Sci Rep*. 2015 Aug 4;5(1):8729.
16. Dewavrin J-Y, Abdurrahim M, Blocki A, Musib M, Piazza F, Raghunath M. Synergistic rate boosting of collagen fibrillogenesis in heterogeneous mixtures of crowding agents. *J Phys Chem B*. 2015 Mar 26;119(12):4350–8.
17. Kumar P, Satyam A, Fan X, Rochev Y, Rodriguez BJ, Gorelov A, et al. Accelerated Development of Supramolecular Corneal Stromal-Like Assemblies from Corneal Fibroblasts in the Presence of Macromolecular Crowders. *Tissue Eng Part C Methods*. 2015 Jul;21(7):660–70.
18. Prewitz MC, Stißel A, Friedrichs J, Träber N, Vogler S, Bornhäuser M, et al. Extracellular matrix deposition of bone marrow stroma enhanced by macromolecular crowding. *Biomaterials*. 2015 Dec 11;73:60–9.
19. Benny P, Badowski C, Lane EB, Raghunath M. Making More Matrix: Enhancing the Deposition of Dermal–Epidermal Junction Components In Vitro and Accelerating Organotypic Skin Culture Development, Using Macromolecular Crowding. *Tissue Eng Part A*. 2015 Jan 9;21(1–2):183–92.
20. Lee MH, Goralczyk AG, Kriszt R, Ang XM, Badowski C, Li Y, et al. ECM microenvironment unlocks brown adipogenic potential of adult human bone marrow-derived MSCs. *Sci Rep*. 2016 Aug 17;6(1):21173.
21. Satyam A, Kumar P, Cigognini D, Pandit A, Zeugolis DI. Low, but not too low, oxygen tension and macromolecular crowding accelerate extracellular matrix deposition in human dermal fibroblast culture. *Acta Biomater*. 2016 Oct;44:221–31.
22. Cigognini D, Gaspar D, Kumar P, Satyam A, Alagesan S, Sanz-Nogués C, et al. Macromolecular crowding meets oxygen tension in human mesenchymal stem cell culture - A step closer to physiologically relevant in vitro organogenesis. *Sci Rep*. 2016 Aug 1;6:30746.
23. Kumar P, Satyam A, Cigognini D, Pandit A, Zeugolis DI. Low oxygen tension and macromolecular crowding accelerate extracellular matrix deposition in human corneal fibroblast culture. *J Tissue Eng Regen Med*. 2017;(March 2017):6–18.
24. Patrikoski M, Lee MHC, Mäkinen L, Ang XM, Mannerström B, Raghunath M, et al. Effects of Macromolecular Crowding on Human Adipose Stem Cell Culture in Fetal Bovine Serum, Human Serum, and Defined Xeno-Free/Serum-Free Conditions. *Stem Cells Int*. 2017;2017:6909163.
25. Magno V, Friedrichs J, Weber HM, Prewitz MC, Tsurkan M V., Werner C. Macromolecular crowding for tailoring tissue-derived fibrillated matrices. *Acta Biomater*. 2017 Jun;55:109–19.
26. Ng WL, Goh MH, Yeong WY, Naing MW. Applying macromolecular crowding to 3D bioprinting: fabrication of 3D hierarchical porous collagen-based hydrogel constructs. *Biomater Sci*. 2018;6(3):562–74.
27. Graceffa V, Zeugolis DI. Macromolecular crowding as a means to assess the effectiveness of

chondrogenic media. *J Tissue Eng Regen Med.* 2018 Dec 14;term.2783.

28. Gaspar D, Fuller KP, Zeugolis DI. Polydispersity and negative charge are key modulators of extracellular matrix deposition under macromolecular crowding conditions. *Acta Biomater.* 2019 Apr;88:197–210.